JOURNAL OF COMPUTATIONAL PHYSICS 104, 444-450 (1993)

Explicit Streamline Method for Steady Flows of Non-Newtonian Matter: History-Dependence and Free Surfaces

S. G. CHUNG

Department of Physics, Western Michigan University, Kalamazoo, Michigan 49008

AND

K. KUWAHARA

The Institute of Space and Astronautical Science, 3-1-1 Yoshinodai, Sagamihara, Kanagawa 229, Japan

Received April 3, 1991; revised December 12, 1991

A new finite-difference method involving a streamline coordinate is developed for analyzing two-dimensional steady non-Newtonian flows with history dependence. The boundary of the material is partially free and partially confined. The proposed method is neither the method of stream function nor the use of convected reference frame. It simply regards streamline as an independent coordinate, thereby retaining the merits of both the Eulerian and Lagrangian schemes. The efficiency of the method is demonstrated in examples of several models' matter steadily discharging from a slit into a free space. © 1993 Academic Press, Inc.

I. INTRODUCTION

This paper describes a new computational method for solving steady two-dimensional flows of non-Newtonian matter with free surfaces and history dependence. The idea was reported elsewhere [1], but the example that was given did not include free surfaces and history-dependence and, hence, did not demonstrate the major advantages of the new method. The idea is to rewrite the basic equations of a material flow in terms of a streamline coordinate. Similar ideas were examined before in various circumstances by Duda and Vrentas [2], Pearson [3], Papanastasiou *et al.* [4], and Luo and Tanner [5]. The former two concern Newtonian fluid and the latter two are streamlined finite element formulations for general complex flows, particularly viscoelastic liquids with memories. These studies revealed a certain merit of the streamline approach to material flows with free surfaces and history dependences. The basic idea of all of these methods resides in an iterative correction of streamline geometry. In the proposed method, we go one step further and regard the streamline as an independent coordinate.

In this paper, we fully explore the efficiency of the streamline coordinate method for analyzing steady flows of complex non-Newtonian matter with free surfaces and history-dependence. In the standard Eulerian method, the coordinates, Cartesian or natural (general), are time independent and mesh points are fixed in space. The streamlines do not necessarily follow mesh points, and therefore integrations along the streamlines to obtain history-dependent quantities can be accurately accomplished only with considerable difficulty. On the other hand, *the streamlines in the present method are by definition always through mesh points.* The motion along a streamline of number m and the time independent coordinates (x, m) are dynamically connected through a new field variable $y(x, m)$. The method is not equivalent to the stream function method, which is simply a potential (scalar or vector) description of the velocity field, and does not imply an ingenious choice of coordinates or mesh points for problems with free surface and/or history dependence. Moreover, as we shall see, the main part of the calculation does not require determination of the streamline positions, $y(x, m)$, but these can be easily found once the velocity fields are solved. This is particularly attractive for problems with free surfaces because, unlike in the conventional method, *we do not need to know the actual positions of the free surfaces during the course of calculations.* No matter what the geometry of confining walls and no matter where the free surfaces, the boundary geometry is always rectangular in the calculational space (x, m).

Computationally, we start with the standard Eulerian finite difference method with natural or general coordinates and modify it so as to meet our formulation [6, 7]. This is to realize a steady flow as a series of transient states, under the expectation that in a low (effective) Reynolds number flow, a strong nonlinearity arising from the present formu-

0021-9991/93 $5.00

lation in addition to non-Newtonian character and/or history-dependence, will not cause numerical instabilities. In fact, we find that our streamline coordinate method is unexpectedly stable. The present method appears to have nearly maximum efficiency for analyzing complex two-dimensional flows with free surfaces and history dependence.

We have organized the paper as follows. In the next section, basic equations are presented for a model Bingham-like material in terms of a streamline coordinate. In Section III, boundary conditions, particularly of free surfaces, are discussed. Section IV describes numerical procedures and some results. Finally, in Section V some concluding remarks are given, especially on a certain difference between two-dimensional and three-dimensional formulations of the new method.

After the completion of this work, we have noticed several papers [11–13]. Ghosh and Kikuchi presented finite-element arbitrary-Lagrangian–Eulerian description of some metal deformation processes. The idea is to introduce grid points which will be close to Lagrangian mesh points when Lagrangian meshes are appropriate but will be homogeneously distributed in the places where Lagrangian meshes are severely distorted, thereby avoiding numerical singularities and inaccuracies associated with the so-called updated Lagrangian method. On the other hand, Hoysan and Steif presented a streamline-based method for steady metal-forming processes. Their idea appears to be the two-dimensional version of that of Pearson [3] in three dimensions. These methods and our method are more or less different in detail but have a common point that they struggle for a best compromise between Eulerian description and Lagrangian descriptions.

It is emphasized that the main goal of this paper is to develop a new efficient method. We must admit that the constitutive equations in the next section, particularly for history dependence, are not quite realistic but do represent essential aspects of nonlinearity and history dependence. A more realistic history dependence model for a specific material as well as a more realistic treatment of the material surface and their accurate and systematic numerical analysis are now on-going and will be reported elsewhere.

II. BASIC EQUATIONS

Let us consider an incompressible two-dimensional flow of Bingham material with free surface and history dependence. The basic equations give

$$\frac{\partial u_i}{\partial x_i} = 0 \tag{1a}$$

$$\frac{\partial u_i}{\partial t} + u_j \frac{\partial u_i}{\partial x_j} = -\frac{\partial P}{\partial x_i} + \frac{\partial}{\partial x_j}(2\nu e_{ij}) \tag{1b}$$

$$\Delta P = \frac{\partial}{\partial x_i}\frac{\partial}{\partial x_j}(2\nu e_{ij}) - \frac{\partial}{\partial x_i}\left[u_j \frac{\partial u_i}{\partial x_j}\right] - \frac{\partial}{\partial t}\frac{\partial u_i}{\partial x_i}, \tag{1c}$$

where the effective kinematic viscosity ν is in general a functional of the strain-rate tensor e_{ij} (see Fig. 1). We assume

$$\nu = \begin{cases} \nu_{\min} & \text{for} \quad e > e_{cr}(\xi) \\ \nu_{\max} + (\nu_{\min} - \nu_{\max})\, e/e_{cr}(\xi) & \text{for} \quad e \leqslant e_{cr}(\xi). \end{cases} \tag{2}$$

In Eq. (2), $e \equiv \sqrt{2e_{ij}e_{ji}}$, $e_{cr}(\xi) \equiv \sigma_y(\xi)/\nu_{\min}$, where the yield stress σ_y is a function of the accumulated deformation (strain) ξ defined by

$$\xi \equiv \prod_n \left[1 + e\frac{\Delta l}{u}\right] - 1 = \prod_n \left[1 + e\frac{\Delta x_i}{u_i}\right] - 1$$
$$\approx \sum_n e\frac{\Delta x_i}{u_i} = \sum_n e\,\Delta t_n, \tag{3}$$

where Δl is a line element along a fluid particle trajectory, an integer n represents a discretized cell or line segment along a streamline, and $\Delta t_n = \Delta x_i/u_i$ is a transit time. It is noted that although Eq. (3) is correct also for a non-steady case, i.e., the deformation field $\xi(\mathbf{r})$ can in general be time dependent, a time-dependent history dependent problem would require a more formidable computational capability. It is also noted that Eq. (2) looks different from the standard definition of a Bingham fluid, where for large strain rates the material becomes less viscous:

$$\begin{aligned} &\nu = \nu_{\min} + \sigma_y/e \qquad \text{for} \quad |\sigma_{ij} + P\delta_{ij}| > \sigma_y \\ &e_{ij} = 0 \qquad\qquad\qquad\quad \text{otherwise.} \end{aligned} \tag{4}$$

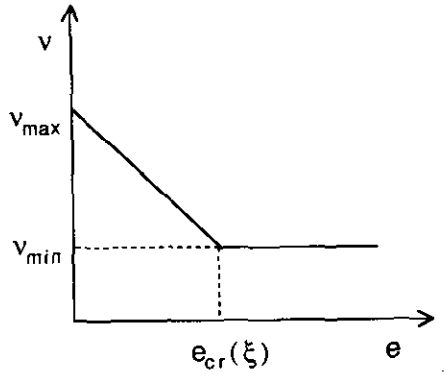

FIG. 1. Dependence of the kinematic viscosity ν on the magnitude of strain-rate e. Note that the relationship is local, depending on the deformation field ξ.

The physical effects of Eqs. (2) and (4) are, however, essentially the same. Since a large stress implies a large strain rate, Eq. (4) means that the effective viscosity ν approaches $\nu_{\min}$ for large strain rates, and increases with decreasing strain rates, reaching $e_{ij}=0$ at some critical value of ν. Equation (2) describes such a behavior of ν and is easily handled numerically. Furthermore, Eq. (2) is more realistic than the standard Bingham model. See Ellwood *et al.* for a modified Bingham model [8].

Now consider a model history-dependent property described by (cf. Fig. 2).

$$\sigma_y(\xi)=\begin{cases}\sigma_{\min} & \text{for} \quad \xi \geqslant \xi_{cr} \\ \sigma_{\max}+(\sigma_{\min}-\sigma_{\max})\,\xi/\xi_{cr} & \text{for} \quad \xi<\xi_{cr}.\end{cases} \tag{5}$$

This increases the yield stress in a region where the deformation is relatively small, which then leads to a larger kinematic viscosity due to Eq. (2) and to a larger portion of nearly rigid motions of materials in the flow field. We are thus considering a strain-softened model Bingham matter.

We now make a coordinate transformation from (x, y) to (x, m) (cf. Fig. 3):

$$y=y(x, m). \tag{6}$$

For any field variables f such as pressure and velocities,

$$\begin{aligned} f_x &\equiv \frac{\partial}{\partial x} f(x, y(x, m))=f_x+f_y y_x \\ f_m &= f_y y_m, \end{aligned} \tag{7}$$

and therefore the differential operators are transformed as

$$\begin{aligned} \partial_x &\to \partial_x-(y_x/y_m)\,\partial_m \\ \partial_y &\to (1/y_m)\,\partial_m. \end{aligned} \tag{8}$$

On the other hand, with the use of $y_x=v/u$ and Eq. (8), we have

$$u_x+v_y=u_x-(y_x/y_m)\,u_m+(1/y_m)\,v_m=(uy_m)_x/y_m. \tag{9}$$

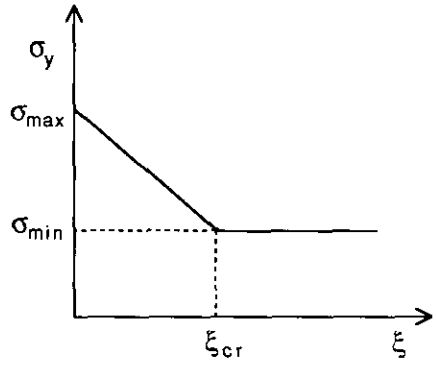

FIG. 2. Dependence of the yield stress σ_y on the deformation ξ.

Therefore, the incompressibility Eq. (1a) gives

$$uy_m=\text{independent of } x \equiv U(m). \tag{10}$$

A convenient choice is to put $U(m)$ equal to the inlet velocity u. This gives at the inlet

$$y=m \tag{11}$$

which defines the position of entering streamlines according to Fig. 3. With Eqs. (8) and (10), the differential operators transform as

$$\begin{aligned} \partial_x &\to \partial_x-(v/U)\,\partial_m \\ \partial_y &\to (u/U)\,\partial_m. \end{aligned} \tag{12}$$

Two things are worth mentioning here about the transformation. First, Eq. (12) can be regarded as a Cartesian to natural coordinate transformation $(x, y) \to (\eta, \zeta)$,[1]

$$\begin{aligned} \partial_x &\to (y_\zeta \partial_\eta-y_\eta \partial_\zeta)/J \\ \partial_y &\to (-x_\zeta \partial_\eta+x_\eta \partial_\zeta)/J, \end{aligned} \tag{13}$$

where $J \equiv x_\eta y_\zeta-x_\zeta y_\eta$. Indeed the transformation (12) is realized by putting

$$\eta=x \quad \text{and} \quad \zeta=m \tag{14}$$

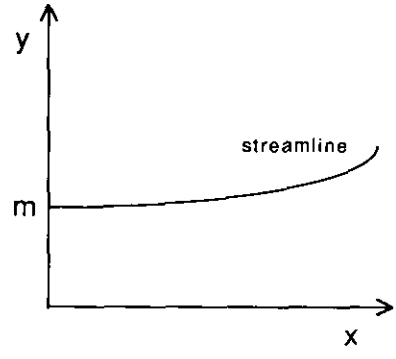

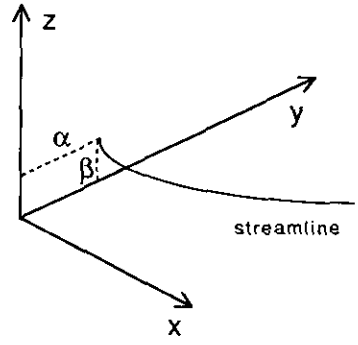

FIG. 3. Streamline geometry in two dimensions (top) and three dimensions (bottom).

in Eq. (13). Unlike the standard natural coordinate method, however, the transformation (12) is dynamical, i.e., its Jacobian is time dependent. Second and more importantly, the transformation coefficients involve velocity fields alone, and therefore, the transformed equations of motion do not explicitly involve the new unknown $y(x, m)$. The free surface condition enters into the problem through a boundary condition which is, as we will see, again expressible in terms of velocities and pressure only. As a result, the numerical procedures are the same as in the standard Eulerian finite difference method, except that the transformed equation of motion and Poisson equation for pressure are now highly nonlinear in velocities. The high nonlinearity has probably been the main obstacle to utilization of this otherwise quite natural idea of using a streamline coordinate for steady non-Newtonian flows with free surfaces and history dependence.

The streamline position $y(x, m)$ of the material can be found by solving the Poisson equation,

$$\begin{aligned}(\partial_{xx}+\partial_{mm})\,y &= (y_x)_x+(y_m)_m \\ &= (v/u)_x+(U/u)_m. \end{aligned} \tag{15}$$

In this way, the present method enables us to determine the streamlines and free material surfaces with ease. An easy determination of streamlines is obviously a benefit in treating history-dependent materials.

III. BOUNDARY CONDITIONS

We have two types of boundaries, rigid walls and free surfaces. At the rigid walls, we impose no-slip conditions, namely $u=v=0$. A free-slip case was examined before [1]. A more general condition at the rigid walls may be appropriate for certain complex processes.

As for free surfaces, two different treatments are known. One is due to Harlow and Welch [9] in the analysis of transient viscous incompressible flows. This is to determine velocities at the free surface from the incompressibility condition, Eq. (1a), and the pressure is simply assumed to be that of the applied external pressure. The other is due to Papanastasiou *et al.* [4] in the streamlined finite element formulation. They require that both the shear stress and normal stress in the absense of surface tension should be zero at the free surface, apart from a uniform pressure:

$$\sigma_{tn}=0 \tag{16a}$$

$$-P+\sigma_{nn}=0. \tag{16b}$$

It is noted that condition (16) is precise, while the condition of Harlow and Welch is an approximation, because pressure can be discontinuous at free surfaces. It is also noted that the conditions (16) are the surface version of the Navier–Stokes equation. One more equation necessary to evaluate velocity and pressure at the surfaces is the mass equation (1b). Equations (16) and (1b) determine the normal gradients u_m, v_m and pressure at the free surfaces. Consulting Fig. 4, we have

$$\begin{aligned} e_{tn} &= (-\sin\theta\partial_x+\cos\theta\partial_y)(u\cos\theta+v\sin\theta) \\ &= (-uvu_x-v^2v_x+u^2u_y+uvv_y)/(u^2+v^2), \\ e_{nn} &= (-\sin\theta\partial_x+\cos\theta\partial_y)(-u\sin\theta+v\cos\theta) \\ &= (v^2u_x-uvv_x-uvu_y+u^2v_y)/(u^2+v^2). \end{aligned} \tag{17}$$

With the use of Eqs. (12) and (17), condition (16) becomes

$$\begin{aligned} &-(uvu_x+v^2v_x)/(u^2+v^2)+(uu_m+vv_m)/U=0 \\ &-\frac{P}{2v}+(v^2u_x-uvv_x)/(u^2+v^2)+(-vu_m+uv_m)/U=0. \end{aligned} \tag{18}$$

Solving Eq. (18), together with Eq. (1b), we have

$$\begin{aligned} u_m &= \frac{U}{u}\left[u_x+u(-u^3u_x+v^3v_x)/(u^2+v^2)^2\right] \\ v_m &= U(-u^3u_x+v^3v_x)/(u^2+v^2)^2 \\ P &= -2uv(uu_x+vv_x)/(u^2+v^2). \end{aligned} \tag{19}$$

An important remark here is that although $U=0$ at free surfaces and the transformation coefficients u/U and v/U are certainly singular there, that does not necessarily mean a real singularity. This is because these coefficients always appear in combination with the operator ∂_m and the derivatives u_m, v_m, and P_m are all vanishing like U at the free surfaces, as is seen from Eq. (19). One can easily show that $P_m \propto U$ at the free surfaces from Eq. (1b).

The velocity profile at the inlet should be given. In a Newtonian case, it is the fully developed channel flow with a unit total flow:

$$\begin{aligned} u_{\text{inlet}} &= 6(y-y_{\min})(y_{\max}-y)/(y_{\max}-y_{\min})^2 \\ v_{\text{inlet}} &= 0, \end{aligned} \tag{20}$$

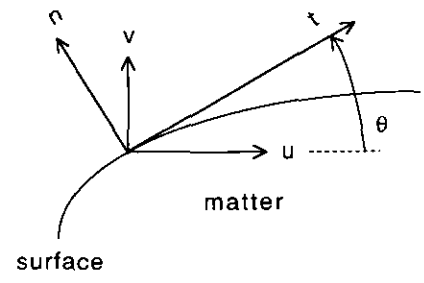

FIG. 4. Suraface geometry.

where y_{min} and y_{max} are, respectively, the positions of lower and upper plates. In the case of a Bingham fluid, a fully developed plug flow is used. As for a history-dependent case, we take the same plug flow at the inlet, assuming that a history dependence is suddenly switched on at the inlet. The velocity profile of the plug flow can also be found analytically by solving an ordinary differential equation,

$$vu_y = \alpha y, \tag{21}$$

together with Eq. (2) with $e_{cr}(\xi) = \sigma_{min}/v_{min}$, although the expression is rather lengthy and we will not write it down here. The constant, α, is related to the total amount of flow. As for the velocity boundary condition at the outlet, we use a simple linear extrapolation.

IV. CALCULATIONAL PROCEDURE AND SAMPLE RESULTS

The sequence of events by which the configuration is advanced from one time step to the next is basically that of the standard Eulerian method. Starting with velocity fields known either as a result of the previous cycle or from the initial conditions, we proceed as follows:

(A) Calculate the relative deformation field ξ by Eq. (3).

(B) Calculate the yield stress field $\sigma_y(\xi)$ by Eq. (5), given the material constants.

(C) Calculate the viscosity field v by Eq. (2), given the material constants.

(D) To solve the pressure Poisson equation (1c), we must avoid a difficulty arising from a possible violation of the Green's theorem which states that, putting the right-hand side of Eq. (1c) as ϕ [10],

$$\int_s \phi \, ds - \int \frac{\partial P}{\partial n} \, dl = 0. \tag{22}$$

We expect on physical grounds that our choice of the Navier–Stokes equation (1c) as a pressure boundary condition at other than free surfaces, together with physically meaningful velocity boundary conditions, would satisfy the Green's theorem to a good approximation. The results of our numerical calculations support this idea. We also note that, following Harlow and Welch [9], the MAC method, the last term in Eq. (1c) is expressed as an advance time difference and then the future term is equated to zero,

$$-\frac{\partial}{\partial t}\frac{\partial u_i}{\partial x_i} \approx -\frac{1}{\Delta t}\left[\left[\frac{\partial u_i}{\partial x_i}\right]^{n+1} - \left[\frac{\partial u_i}{\partial x_i}\right]^{n}\right]$$

$$\approx \frac{1}{\Delta t}\left[\frac{\partial u_i}{\partial x_i}\right]^{n}, \tag{23}$$

where the present and next steps are denoted by indices n and $n+1$. Clearly, the idea is to determine the pressure in order for the velocity to satisfy the incompressibility condition.

(E) Considering the strong nonlinearity of the present formulation, we use an implicit method for evaluating the velocity field in the next step. That is, we write Eq. (1b) as

$$\frac{u_i^{n+1} - u_i^n}{\Delta t} = -u_j^n \frac{\partial u_i^{n+1}}{\partial x_j} - \frac{\partial P^n}{\partial x_j} + 2\frac{\partial}{\partial x_j}(v^n e_{ij}^{n+1}) \tag{24}$$

and solve for u_i^{n+1}. It should, of course, be understood that all the quantities are in terms of (x, m) coordinates and the operators should be transformed using Eq. (12).

This, then, completes one cycle. As is pointed out in Section II, the basic equations (1) do not explicitly depend on $y(x, m)$, the actual position of streamlines. For a steady problem, therefore, $y(x, m)$ does not have to be evaluated at each step. One needs to solve the Poisson equation (15) only once after the iterational calculation reaches a steady state. The Poisson equation (15) can be solved by the same procedure as for the pressure, with $y_x = v/u$ and $y_m = U/u$ giving the boundary conditions. A penalty for this nice mathematical structure of the streamline method is a strong nonlinearity which, however, turns out to be less troublesome than is expected.

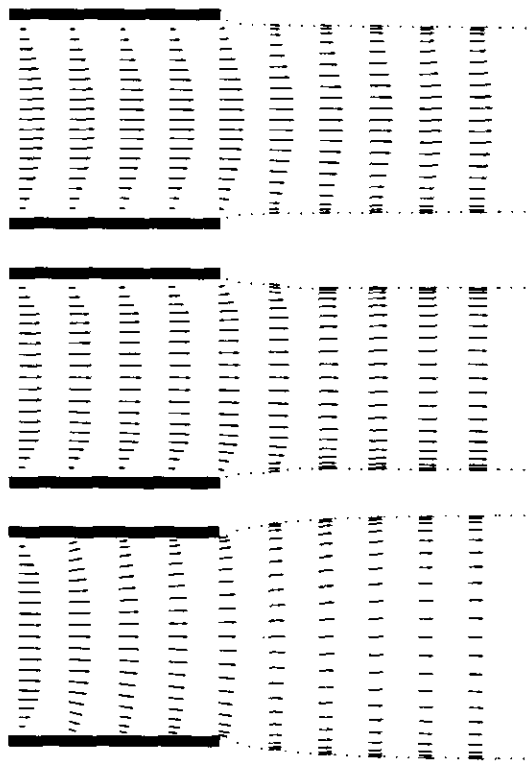

FIG. 5. Calculated flow patterns for, from top to bottom, a Newtonian fluid, a modified Bingham fluid, and a strain-softened Bingham fluid.

Using the streamline coordinate method, the flow dynamics of some two-dimensional matter discharging from the parallel plates into a free space is analyzed. Figure 5 shows calculated flow patterns for, from top to bottom, a Newtonian fluid, a modified Bingham fluid, and a strain-softened Bingham fluid. The relevant parameters are $\Delta t = 0.003$, $\Delta x = \Delta m = 0.05$, $\nu_{\min} = 0.01$, $\nu_{\max} = 0.1$, $\sigma_{\min} = 0.05$, $\sigma_{\max} = 0.2$, and $\xi_{cr} = 10$. Corresponding pressure contours are shown in Fig. 6. Viscosity contours corresponding to Fig. 5 middle and Fig. 5 bottom respectively are shown in Fig. 7 top and Fig. 7 bottom. The contours of the accumulated deformation as defined by Eq. (3) are shown in Fig. 8. This deformation is responsible for the yield stress $\sigma_y(\xi)$, Eq. (5), and hence for the viscosity change from Fig. 7 top to Fig. 7 bottom. To obtain these results, iterations were continued until the following convergence criteria was fulfilled:

$$\sum_{i,j} |u^n(i,j) - u^{n+1}(i,j)| \Big/ \sum_{i,j} |u^n(i,j)| < 10^{-6}. \qquad (25)$$

A plug flow featuring the Bingham fluid is clearly seen in Fig. 5 middle. A difference between Fig. 5 middle and Fig. 5 bottom is in the lateral (y) width of the material at the outlet; the latter swells relative to the former. On the other hand, there is no such difference between Fig. 5 top and Fig. 5 middle. Qualitatively, comparing velocities and viscosities, one easily finds that the viscosity responsible for the lateral width at the outlet is that near the parallel plates. In the Bingham case, the relevant viscosity, which connects the main part of the flow to the rest of the flow and to the resistive walls, is as small as in the Newtonian case. The main part, therefore, moves with relatively small resistance, and hence small momentum loss, into the free space and is accompanied by a subsequent acceleration of the rest of the material, which then shrinks in the lateral direction due to incompressibility. In the history-dependent case, on the other hand, the relevant viscosity is rather large, implying that the whole material now moves rigidly with a relatively large momentum loss. As a result, the uniform speed is relatively small at the outlet, giving rise to a relatively large lateral width. This argument then suggests that the

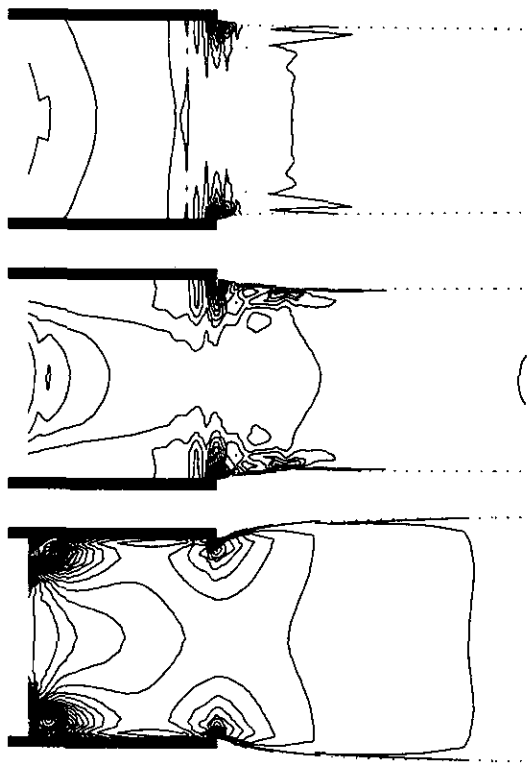

Fig. 6. Isobars corresponding to the cases (top), (middle), and (bottom) in Fig. 5 are shown in top, middle, and bottom, respectively. Pressure interval between lines is 0.02. Pressure is zero at the free surface and shows a large minimum right after the exits near the corner. A structure near the inlet in the cases (middle) and (bottom) signifies a quick development of the plug flow from the Newtonian inlet flow.

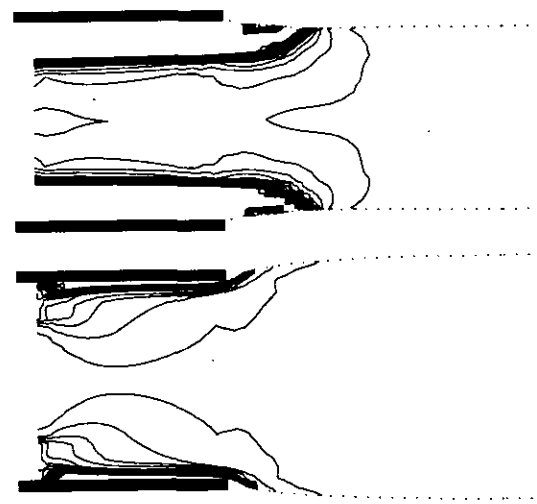

FIG. 7. Viscosity contours corresponding to the cases (middle) and (bottom) in Fig. 5 are shown in top and bottom, respectively. Viscosity interval between lines is 0.005. Viscosity changes rapidly from its minimum 0.01 near the wall to its maximum 0.1 in the rest of the material through a thin region.

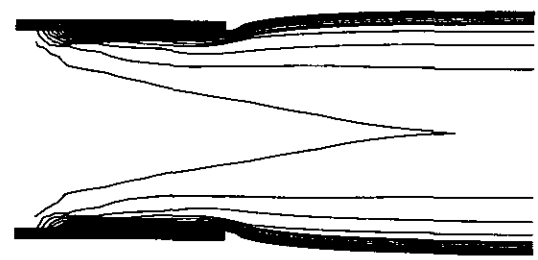

FIG. 8. Contours of the accumulated deformation ξ. It is zero at the inlet and increases down the stream and toward the no-slip walls. The interval between lines is 1.0.

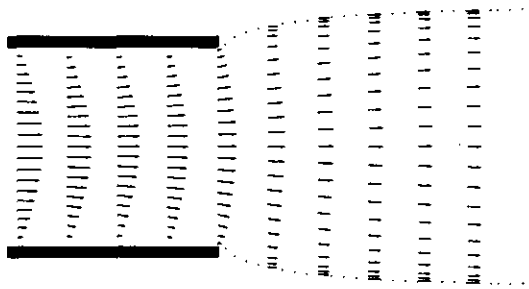

FIG. 9. Calculated flow pattern for a Newtonian fluid with $v = 0.1$.

Newtonian case with $v = v_{max}$ will exhibit a larger lateral width at the outlet as in Fig. 5 bottom. As is seen in Fig. 9, this is indeed the case, although the history dependence imposes some difference between Fig. 5 bottom and Fig. 9.

V. CONCLUDING REMARKS

In this paper, we have described a new computationally efficient method for analyzing steady non-Newtonian flows with free surfaces and history dependence. In our method, the streamlines always pass through mesh points and the determination of velocities and pressure, and that of streamlines, are separated from each other. This is clearly a benefit in solving problems with free surfaces and history dependence.

We should also mention that there are some underlying assumptions or limitations to the streamline coordinate method. First, we have assumed that no circulation exists in the flow. Second, we have also assumed that the high-nonlinearity in the transformed basic equations would not cause any numerical instabilities. These assumptions are, however, reasonable because our goal is to analyze the flow dynamics of history-dependent non-Newtonian matter with a relatively low effective Reynolds number. Moreover, the first assumption, we believe, could be removed without much difficulty.

Finally, we note that the present method essentially relies on the two-dimensionality. In three dimensions, two parameters α and β are necessary to characterize a streamline (cf. Fig. 3):

$$y = y(x, \alpha, \beta); \quad z = z(x, \alpha, \beta). \tag{26}$$

Denoting the x-component of the inlet velocity by $U(\alpha, \beta)$, one can show that the incompressibility condition now gives, instead of the corresponding two-dimensional Eq. (10),

$$u(y_\alpha z_\beta - y_\beta z_\alpha) = U(\alpha, \beta). \tag{27}$$

Equation (27) alone is, of course, not sufficient to determine each element of the Jacobian $\partial(y, z)/\partial(\alpha, \beta)$. As a result, the transformed basic equations are no more free from the new field variables y and z. Some innovations are thus called for to preserve the nice mathematical structure of the two-dimensional streamline coordinate formulation. Nevertheless, the computational efficiency of the streamline coordinate method should apply in any dimension for the accurate analysis of the flow dynamics of non-Newtonian matter with free surfaces and history dependence.

ACKNOWLEDGMENT

We thank Owen Richmond for critically reading the manuscript and for helpful suggestions.

REFERENCES

1. S. G. Chung, S. C-Y. Lu, and O. Richmond, *Phys. Rev. A* **39**, 2728 (1989).
2. J. L. Duda and J. S. Vrentas, *Chem. Eng. Sci.* **22**, 855 (1967).
3. C. E. Pearson, *J. Comput. Phys.* **42**, 257 (1981).
4. A. C. Papanastasiou, C. W. Macosko, and L. E. Scriven, in *Finite Elements in Fluids*, edited by R. H. Gallagher *et al.* (Wiley, London, 1985), Vol. 6, p. 263; A. C. Panastasiou, L. E. Scriven, and C. W. Macosko, *J. Non-Newtonian Fluid Mech.* **22**, 271 (1987).
5. X.-L. Luo and R. I. Tanner, *J. Non-Newtonian Fluid Mech.* **21**, 179 (1986); **22**, 61 (1986); **31**, 143 (1989).
6. *Handbook of Fluid Mechanics*, edited by Japan Association of Fluid Mechanics (Maruzen, Tokyo, 1987).
7. D. Takahashi, K. Kuwahara, and R. Himeno, unpublished.
8. K. R. Ellwood, G. C. Gerogiou, A. C. Papanastasiou, and J. O. Wilkes, *J. Rheol.* **34**, 787 (1990).
9. F. H. Harlow and T. E. Welch, *Phys. Fluids* **8**, 2182 (1965).
10. P. J. Roach, *Computational Fluid Dynamics* (Hermosa, Albuquerque, NM, 1976), p. 184.
11. S. Ghosh, *J. Mater. Shaping Technol.* **8**, 53 (1990).
12. S. Ghosh and N. Kikuchi, preprint.
13. S. F. Hoysan and P. S Steif, preprint.